Arabian Journal of Chemistry (2017) **10**, S2429–S2435

King Saud University

Arabian Journal of Chemistry

www.ksu.edu.sa
www.sciencedirect.com

ORIGINAL ARTICLE

Luminescence quenching of tris(4,4′-dinonyl-2,2′-bipyridyl) ruthenium(II) cation with phenolate ions in DMSO

Sheeba Daniel, George Allen Gnana Raj *

Department of Chemistry and Research Centre, Scott Christian College (Autonomous), Nagercoil 629003, Tamil Nadu, India

Received 11 March 2013; accepted 4 September 2013
Available online 13 September 2013

KEYWORDS

Luminescence quenching;
Stern–Volmer equation;
Photooxidation of phenols;
Photoinduced electron transfer;
Structural effects

Abstract The photoredox reactions of biologically important phenols (*p*-coumaric acid, ferulic acid, thymol, quercetin and gallic acid) with the excited state $[Ru(nbpy)_3]^{2+}$ (nbpy = 4,4′-dinonyl-2,2′-bipyridine) complex proceed through photoinduced electron transfer reaction in DMSO and have been studied by luminescence quenching technique. The complex shows absorption and emission maximum at 457 and 628 nm and it shows a lifetime of 804 ns in DMSO. The excited state reduction potential of the complex $E^0_{Ru^{2+*/+}}$ in DMSO is 0.72 V vs Ag/Ag^+. The dynamic nature of quenching is confirmed from the ground state absorption studies. The reductive quenching of $[Ru(nbpy)_3]^{2+}$ by phenolate ions has been confirmed from transient absorption spectra and from the linear variation of $\log k_q$ vs oxidation potential of the phenols. The quenching rate constant, (k_q) is highly sensitive to the availability of active phenolate ions, oxidation potential of the polyphenols, the free energy change (ΔG^0) of the reaction and to the electron transfer distance between the complex and the quencher. Structural effects seem to play an important role in the photoinduced electron transfer reactions in DMSO.

1. Introduction

Polyphenols constitute one of the most common and widespread groups of substances in flowering plants, occurring in all vegetative organs, as well as in flowers and fruits. They are considered as secondary metabolites involved in the chemical defense of plants against predators and in plant-plant interferences. Several thousand plant polyphenols are known, encompassing a wide variety of molecules that contain at least one aromatic ring with one or more hydroxyl groups in addition to other substituents. The biological properties of polyphenols include antioxidant, anticancer, and anti-inflammatory effects (Gianmaria et al., 2011). The antioxidant activity of phenolic compounds is due to their ability to scavenge free radicals, donate hydrogen atoms or electron, or chelate metal cations. Among the variety of phenolic compounds, phenolic acids have attracted considerable interest in the past few years due to their many potential health benefits. The conversion of phenol to phenoxyl radical is of interest to chemists because of its involvement in biologically important processes (Swarnalatha et al., 2011). The one electron oxidation of phenolates to the resulting phenoxyl radical is a key step in the

* Corresponding author. Mobile: +91 9487311237.
E-mail address: allengraj@gmail.com (A.G.R. George).
Peer review under responsibility of King Saud University.

Production and hosting by Elsevier

http://dx.doi.org/10.1016/j.arabjc.2013.09.006
1878-5352

oxidation of phenols. The study of the kinetic and thermodynamic aspects of electron transfer to generate phenoxyl radicals bearing bulky groups in the *ortho*- and *para*-positions may help to understand the different biological roles of phenols.

The photochemistry and photophysics of transition metal complexes containing d^6 electronic configuration, particularly Ruthenium polypyridyl complexes ($[Ru(NN)_3]^{2+}$), have attracted the chemists in the design of light-driven water splitting photoanodes (Brimblecombe et al., 2010; Li et al., 2010; White et al., 2012; Young et al., 2012), molecular probes (Gill and Thomas, 2012; Liao et al., 2012; Tan et al., 2013; Tan et al., 2012), construction of solar cells (Adewale et al., 2012; Chitra et al., 2013; Sannino et al., 2013; Brewster et al., 2011; Tuikka et al., 2011), artificial photosynthesis (Kalyanasundaram and Graetzel, 2010) sensors (Cui et al., 2008; Schmittel and Lin, 2008), molecular machine devices (Balzani et al., 2009; Li et al., 2008) and organic light emitting diodes (Chi and Chou, 2010). This is due to the combination of excellent photophysical and electrochemical properties such as luminescence in solution at room temperature, moderate quantum yield and excited state lifetime, spectroscopically distinguishable metal redox states, tunable electronic properties, ability to undergo energy and electron transfer processes and chemical stability (Campagna et al., 2007; Kavan et al., 2008; Lee et al., 2003; Lo et al., 2008; Siebert et al., 2011; Sun et al., 2010).

The synthesis of Ru(II) complexes with long chain hydrophobic ligands is of great interest in recent years because of their potential applications in thin film devices, sensors, heterogeneous catalysis (Dunn and Zink, 2007; Holder et al., 2005; Metera and Sleiman, 2007) and for the construction of dye sensitized solar cells (Chandrasekharam et al., 2011; Xu et al., 2012; Zhu et al., 2012). The dyes with longer hydrocarbon chains give higher efficiency when used as a sensitizer in dye sensitized solar cells (Mori et al., 2007). Castro and co-workers (Castro et al., 2005) have successfully designed a sensor for hydrocarbon, based on ruthenium(II)-complex, ($[Ru(nbpy)_3]^{2+}$ (nbpy = 4,4′-dinonyl-2,2′-bipyridine)) which is able to detect reversibly and to quantify both aromatic and aliphatic hydrocarbons in aqueous samples.

The excited state properties like emission lifetime, quantum yield, wavelength of emission maximum and redox potentials of $[Ru(bpy)_3]^{2+}$ (bpy = 2,2′-bipyridine) are largely affected by the introduction of electron-donating and electron-withdrawing groups in the 4,4′-position of 2,2′-bipyridine (Rajendran et al., 2001; Rajendran et al., 1997; Swarnalatha et al., 2005). The excited state properties of ruthenium(II)-polypyridine complexes can also be finely tuned by changing the nature of the solvent or medium. The rate of electron transfer from a donor molecule to an acceptor in a solvent is controlled by several factors and the most important of them are the free energy change of the reaction (ΔG^0), the reorganization energy (λ) and the electron transfer distance (d) between the donor and acceptor (Verma et al., 2012). Numerous works have been reported on the importance of the substituent, pH, steric and electronic effects on the photoinduced electron transfer reactions of *ortho*-, *meta*- and *para*-substituted phenolate ions to the excited state Ru(II)-polypyridine complexes in aprotic, protic, mixed solvents and in micelles (Miedlar and Das, 1982; Rajendran et al., 2001; Rajendran et al., 1997; Swarnalatha et al., 2011; Swarnalatha et al., 2005; Thanasekaran et al., 1998; Verma et al., 2012).

Luminescence quenching is an important technique used to obtain adequate information about structure and dynamics of luminescent molecules. It is a process, in which the luminescence intensity of the solute decreases by a variety of molecular interactions such as excited state reactions, molecular rearrangements, energy transfer, ground-state complex formation and collision-quenching (Huili et al., 2012; Matos et al., 2008). The present study concentrates on the quenching behavior of the $[Ru(nbpy)_3]^{2+}$ complex with polyphenols and thymol (quenchers) in DMSO. The transient absorption spectra confirm the electron transfer nature of the reaction of the excited state $[Ru(nbpy)_3]^{2+}$ with polyphenols in DMSO, where the quenching process proceeds through the formation of phenolate ions. Further, the nature of quenching (static or dynamic) is recorded by electronic absorption spectra as well as quenching rate constant.

2. Experimental

2.1. Materials

$RuCl_3.3H_2O$, ligand (4,4′-dinonyl-2,2′- bipyridine) and the quenchers (*p*-coumaric acid, ferulic acid, thymol, gallic acid, quercetin) were purchased from Sigma–Aldrich. HPLC grade solvents were used throughout the study for the synthesis of complex as well as for quenching studies. The complex, $[Ru(nbpy)_3]\ Cl_2$ was synthesized according to the procedure previously described (Castro et al., 2005). Then the complex was treated with sodium tetrafluoroborate to get the BF_4^- salt $[Ru(nbpy)_3](BF_4)_2$.

2.2. Equipments

Samples of the complex, $[Ru(nbpy)_3]^{2+}$ as well as the quenchers in DMSO were freshly prepared for each measurement. Absorption spectra were measured using SYSTRONICS 2203 double beam spectrophotometer. Emission spectra were recorded using JASCO FP-6300 spectrofluorometer. All the sample solutions used for emission and excited state lifetime measurements were deaerated for about 30 min by dry nitrogen gas purging keeping the solutions in cold water to ensure that there is no change in volume of the solution. All the spectral measurements were carried out at 298 K. Excited state lifetime and transient absorption measurements were made with laser flash photolysis technique using an Applied Photophysics SP-Quanta Ray GCR-2(10) Nd:YAG laser as the excitation source (Ramamurthy, 1993). The time dependence of the luminescence decay was observed using a Czerny–Turner monochromator with a stepper motor control and a Hamamatsu R-928 photomultiplier tube. The production of the excited state on exposure to 355 nm was measured by monitoring (pulsed Xenon lamp of 250 W) the absorbance change. Transient spectra were obtained by a point-to-point technique, monitoring the absorbance changes (ΔA) after the flash at intervals of 10 nm over the spectral range 300–700 nm, averaging at least 30 decays at each wavelength.

The redox potential of the complex, $[Ru(nbpy)_3]^{2+}$ and the oxidation potentials of the polyphenols in DMSO medium were determined by cyclic voltammetric technique using CH1604C electrochemical analyzer. A glassy carbon (working electrode), Pt (counter electrode) and (Ag/Ag^+) electrode

(reference electrode) were used for the electrochemical measurements and tetrabutylammonium perchlorate was the supporting electrolyte.

2.3. Luminescent quenching studies

The structure of the ligand and the quenchers used in the present study are shown in Fig. 1. The complex and the quenchers taken in the present study are soluble in DMSO and the excited state life time of the $[Ru(nbpy)_3]^{2+}$ is longer in aprotic solvents than protic one (Castro et al., 2005). DMSO has greater proton affinity than other aprotic solvent like acetonitrile (Astudillo et al., 2007). In DMSO, a hydrogen bonding interaction is established between the phenolic –OH groups of the phenols and the oxygen atom of DMSO (O–H…O), which polarize the O–H bond, making the proton transfer easier than in the case of acetonitrile (Astudillo et al., 2007). This proton transfer yields phenolate ion, which act as quenchers in these photoinduced ET reactions, hence we use DMSO as solvent in this study. The photochemical reduction of $[Ru(nbpy)_3]^{2+}$ complex with these phenolate ions has been studied by the luminescence quenching technique. The sample solutions were purged carefully with dry nitrogen for 30 min. The luminescence measurements (Fig. 2) were performed at different quencher concentrations and the quenching rate constants, k_q, were determined from Stern–Volmer plots (Fig. 3) using the equation given below (Lakowicz, 2006).

$$I_0/I = 1 + k_q\tau_0[Q] \quad (1)$$

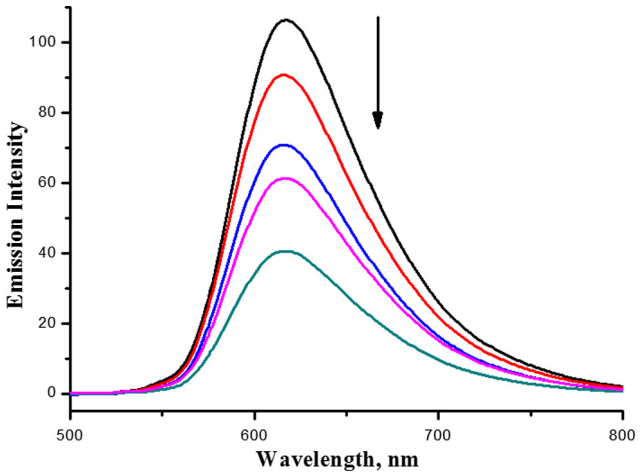

Figure 2 The change in emission intensity of $^{*}[Ru(nbpy)_3]^{2+}$ with different concentrations of gallic acid (2×10^{-4}–1.4×10^{-3}) in DMSO.

Where I_0 and I are the emission intensities in the absence and presence of quencher respectively and τ_0 is the emission lifetime of $[Ru(nbpy)_3]^{2+}$ in the absence of quencher.

3. Results and discussion

3.1. Electronic spectra and luminescent life time

The absorption spectrum of $[Ru(nbpy)_3]^{2+}$ shows a high energy absorption at 286 nm corresponding to the ligand

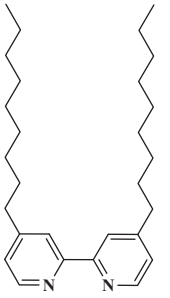

4,4'-dinonyl-2,2'-bipyridine

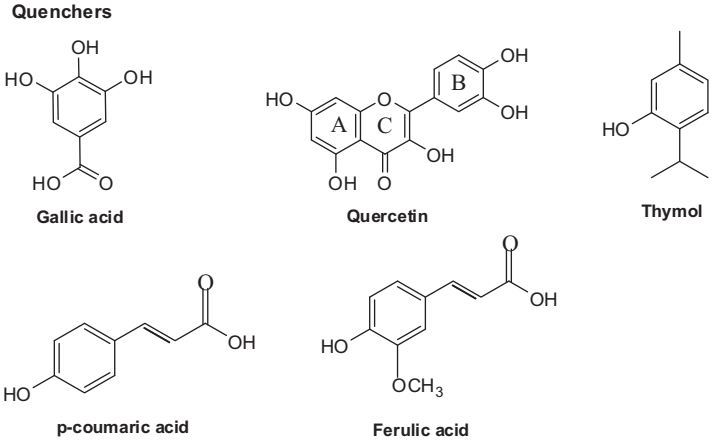

Figure 1 Structure of ligand and quenchers.

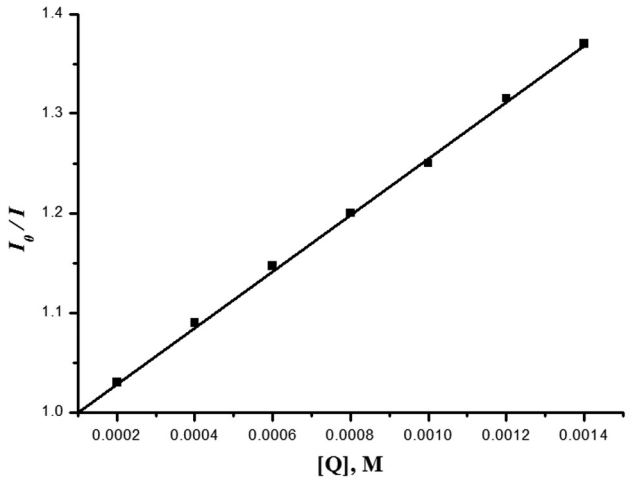

Figure 3 Stern–Volmer plot for the reductive quenching of $^{*}[Ru(nbpy)_3]^{2+}$ with *p*-coumaric acid in DMSO.

centered π–π^* transition and a low energy absorption at 457 nm assigned to the $d\pi$–π^* metal to ligand charge transfer (MLCT) transition. The MLCT involves electronic excitation from the metal orbital [$d\pi$ (Ru)] to the ligand centered acceptor π^* orbitals (ligand). The $[Ru(nbpy)_3]^{2+}$ complex shows an emission maximum at 625 nm and has an excited state lifetime at 804 ns in DMSO.

3.2. Redox potential

The ground state reduction potential of the Ru(II) complex in DMSO is −1.37 V vs Ag/Ag^+ electrode. The redox potentials of excited state couples are calculated from the potential of the ground state couples and the zero–zero energy, $E_{0\text{–}0}$ (found to be 2.1 eV) (Swarnalatha et al., 2005). The excited state redox potential of the complex $\left(E_{Ru}^{2+*/+}\right)$ is 0.72 V vs Ag/Ag^+. The free energy change (ΔG^0) values are calculated from the excited state redox potential of [Ru(4,4′-dinonyl-2,2′-bipyridine)$_3$]$^{2+}$ and oxidation potentials of polyphenols. The experimental bimolecular quenching rate constant (k_q) of $^{*}[Ru(nbpy)_3]^{2+}$, oxidation potentials of quenchers vs Ag/Ag^+, and ΔG^0 in DMSO are shown in Table 1.

3.3. Luminescence quenching of $^{*}[Ru(4,4'$-dinonyl-2,2′-bipyridine$)_3]^{2+}$ with phenolate ions

The Stern–Volmer plots for the emission intensity of the photoredox systems (Fig. 3) are found to be linear which indicates that, dynamic quenching is the dominant process and the contribution from static quenching is negligible. In order to check the ground-state complex formation, quenchers are added in increments to the $[Ru(nbpy)_3]^{2+}$ complex in DMSO and the absorption spectra are recorded at different concentrations (Fig. 4). The absorption spectra of the reactants are equal to the sum of the component spectra. There is no significant change in MLCT absorption maxima of $[Ru(nbpy)_3]^{2+}$ in the presence of the quenchers under the present experimental conditions which helps us to conclude that the contribution from the static quenching is negligible here (Swarnalatha et al., 2011).

Table 1 Rate constants (k_q), oxidation potential of quenchers vs Ag/Ag^+ (E^0_{oxd}) and free energy changes (ΔG^0) for the reductive quenching of $[Ru(nbpy)_3]^{2+}$ with the quenchers in DMSO.

Quencher	k_q (M^{-1} s^{-1})	E^0_{oxd} vs Ag/Ag^+ (V)	ΔG^0 (eV)
Phenol	1.4×10^8	0.78	0.06
p-Coumaric acid	3.1×10^8	0.67	−0.047
Ferulic acid	8.7×10^8	0.51	−0.212
Thymol	1.24×10^9	0.41	−0.307
Quercetin	2.48×10^9	0.30	−0.422
Gallic acid	6.21×10^9	0.082	−0.639

The k_q values for gallic acid, quercetin and thymol are 6.21×10^9, 2.48×10^9 and 1.24×10^9 M^{-1} s^{-1}, respectively, whereas ferulic acid and *p*-coumaric acid record 8.7×10^8, 3.1×10^8 M^{-1} s^{-1}. For the sake of comparison of the quenching efficiencies, substituent effect and ΔG^0 of the polyphenols with this complex, we have done this luminescent study with phenol also and the results are discussed here. Phenol shows the least k_q of 1.4×10^8 M^{-1} s^{-1}. Miedlar and Das reported this type of least k_q value for phenol in the photoredox reactions of $[Ru(bpy)_3]^{2+}$. The availability of phenolate ions is more with respect to gallic acid (Angelique et al., 2010) due to the presence of three phenolic –OH groups, acts as an efficient quencher compared to the other polyphenols taken in the present study. Quercetin has two different pharmacophores, the catechol group (ring B) and the benzo-γ-pyrone derivative (ring A and C), of which the catechol moiety is the most reactive one where deprotonation occurs easily (Trouillas et al., 2006). Steric hindrance exerted by the benzo-γ-pyrone derivative at *para*-position of the ring B reduces its quenching efficiency when compared to gallic acid. This steric effect can be ascribed to the increase of electron transfer distance when the reaction occurs between two reactants carrying bulky groups (Swarnalatha et al., 2005). The quenching efficiency of thymol is somewhat lower than quercetin, due to the presence of one phenolic –OH and the isopropyl group at the *ortho*-position of phenol exerting a slight steric hindrance there by reducing the quenching rate constant. The hydroxyl

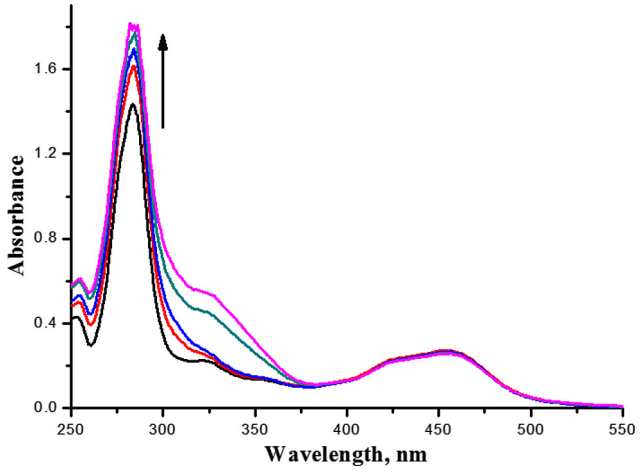

Figure 4 Absorption spectra of $[Ru(nbpy)_3]^{2+}$ in the presence of different concentrations of ferulic acid in DMSO.

derivatives of cinnamic acid (*p*-coumaric acid and ferulic acid) show the smallest k_q values. The –CH=CH–COOH chain at the *para*-position of phenol has electron acceptor properties and the stabilization of the resulting phenolate ion might be increased by electron delocalization. Hence the availability of phenolate ion is much less in *p*-coumaric acid and ferulic acid thus reduces the quenching rate constant. The k_q of ferulic acid is somewhat higher than *p*-coumaric acidformer due to the presence of an electron-releasing methoxy group in the *ortho*-position of the phenol. Here the nature of the substituent in the *ortho*- and *para*-positions of phenols affects the k_q.

The BDE for the phenolic –OH group in gallic acid (75.5 kcal/mol) (Harris et al., 2007), is less than that of the other phenols taken in the present study. Due to this low BDE, gallic acid undergoes ionization easily and acts as the most efficient quencher than quercetin, thymol, ferulic acid, *p*-coumaric acid and phenol. Though quercetin consists of four phenolic –OH groups, the BDE of the catechol group (ring B) is less compared to the phenolic –OH groups in ring A; therefore the catechol group undergoes oxidation easily (Trouillas et al., 2006). The quenching rate constant depends on the number of phenolic –OH groups present in the quencher. As the number of phenolic –OH group increases the quenching rate constant also increases. Here in this study the quenching rate constant for gallic acid is higher than the other phenols, owing to the presence of three phenolic –OH groups.

Phenolate ions containing alkyl groups in the *ortho*-position play an important role in the antioxidant activity of phenols (Lakowicz, 2006). The compounds with two or more electron donating groups have lower oxidation potentials than monosubstituted phenols, although –OH groups have stronger effects than $-OCH_3$ groups (Aleksandra et al., 2007). Here the oxidation potentials of the polyphenols containing electron releasing groups in the *ortho*-position are very low, i.e., ΔG^0 becomes more negative. The ΔG^0 values (Table 1) indicate that all reactions are exergonic except with phenol. The oxidation potential (0.78 V) and ΔG^0 (0.06 eV) of phenol also support the lowest k_q for $[Ru(nbpy)_3]^{2+}$ in DMSO. This is in good agreement with the reported k_q value for luminescent quenching of $[Ru(bpy)_3]^{2+}$ by phenolate ions in aqueous medium at pH 12.5 (Swarnalatha et al., 2005). Gallic acid has a very low oxidation potential (0.082 V) and the ΔG^0 value is more negative (−0.639 eV), hence it undergoes oxidation easily and acts as an efficient quencher compared to the other polyphenols taken in the present study. *p*-coumaric acid shows a high oxidation potential value of 0.67 V and the free energy change is −0.047 eV, recording a very low quenching rate constant. The oxidation potential of ferulic acid (0.51 V) is less than that of *p*-coumaric acid indicating that the former undergoes oxidation easily, and shows somewhat higher k_q than the latter. The oxidation potentials of quercetin and thymol are 0.3, and 0.41 V, respectively and the corresponding ΔG^0 values are −0.422 and −0.307 eV. Thus the k_q values are highly sensitive to the oxidation potential of the quenchers and the ΔG^0 of the reactions.

The k_q also depends on the electron transfer distance between the complex and the quenchers. From MM2 molecular model the radius of gallic acid, quercetin and thymol, are 4.1, 5.93 and 3.9 Å whereas *p*-coumaric acid and ferulic acid show the same radius (4.8 Å). The radius of thymol is less than that of gallic acid, hence the electron transfer distance is less in thymol than gallic acid but the k_q value of gallic acid is superior to thymol due to its lower oxidation potential (0.08 V) and ΔG^0 value (−0.64 eV). Quercetin excerts greater electron transfer distance due to its high radius and it reduces the k_q. The radius of ferulic acid and *p*-coumaric acid seem to be the same but the nature of the substituent ($-OCH_3$) in the former increases the k_q to some extent than the latter. This result concludes that the k_q value depends not only on the ET distance but also on ΔG^0 value.

The reductive quenching of $^*[Ru(nbpy)_3]^{2+}$ by the phenolate ions has been confirmed from the transient absorption spectra (Fig. 5) and from the linear variation of log k_q vs oxidation potential of the phenols (Fig. 6). The band at 510 nm in the transient absorption spectra of the complex with quercetin confirms the reductive nature ($[Ru(nbpy)_3]^+$) of the complex. The behavior of these redox systems can be discussed by a common mechanism depicted in Scheme 1 (Swarnalatha et al., 2005). The reactants diffuse together to form the encounter complex at the closest distance of approach. The electron transfer occurs in this association complex $[^*Ru(NN)_3{}^{2+} \ldots ArO^-]$ resulting in the formation of a caged

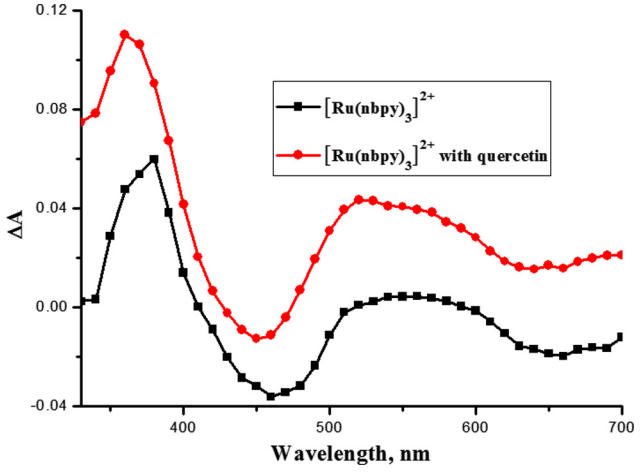

Figure 5 Transient absorption spectra of $[Ru(nbpy)_3]^{2+}$ at 100 ns after 355 nm laser flash photolysis in the absence and presence of 0.0008 M quercetin in DMSO.

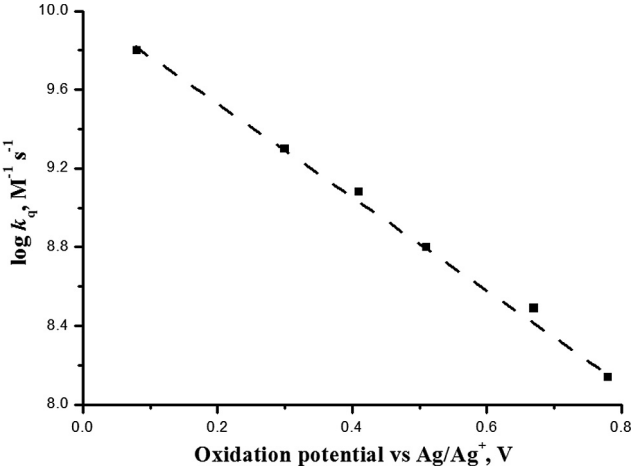

Figure 6 Plot of log k_q vs oxidation potential of quenchers.

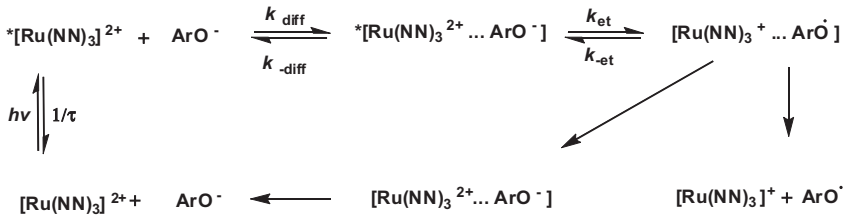

Scheme 1 Mechanism for the electron transfer quenching of $^{*}[Ru(NN)_3]^{2+}$ with ArO^{-}.

pair of radicals or radical ions. These radical ions either escape from the solvent cage to give the redox products or undergo back electron transfer to form original reactants.

4. Conclusion

The present study clearly establishes the luminescence quenching mechanism of photoredox reactions of the $^{*}[Ru(nbpy)_3]^{2+}$ with the polyphenols in DMSO. The k_q depends on the availability of phenolate ions, oxidation potentials of the polyphenols, ΔG^0 values and the electron transfer distance between the $^{*}[Ru(nbpy)_3]^{2+}$ and the quencher. The nature of the substituent in the *ortho*- and *para*-positions affects the quenching rate constant. Gallic acid behaves as an efficient quencher compared to other polyphenols due to the availability of more number of phenolate ions. The oxidation potential and the corresponding free energy change values also confirm the higher rate of quenching for gallic acid than other polyphenols taken in the present study. This study confirms the structural effect on the electron transfer reactions of biologically important phenolate ions with the excited state $^{*}[Ru(nbpy)_3]^{2+}$.

Acknowledgments

One of the authors Sheeba Daniel thanks the Council of Scientific and Industrial Research (CSIR), New Delhi for the award of Senior Research Fellowship and Prof. P. Ramamurthy, Director, National Centre for Ultrafast Processes, University of Madras, Chennai for permitting to do lifetime measurements.

References

Adewale, O., Adeloye, A.O., Olomola, T.O., Adebayo, A.I., Ajibade, P.A., 2012. A high molar extinction coefficient bisterpyridyl homoleptic Ru(II) complex with *trans*-2-methyl-2-butenoic acid functionality: potential dye for dye-sensitized solar cells. Int. J. Mol. Sci. 13, 3511–3526.

Aleksandra, S., Dragan, M., Dejan, S., Marija, T., 2007. Electrochemical behavior and antioxidant and prooxidant activity of natural phenolics. Molecules 12, 2327–2340.

Angelique, C.E., Wanvimol, P., Brett, A.W., Garry, R.B., 2010. Free radicals produced by the oxidation of gallic acid: an electron paramagnetic resonance study. Chem. Cent. J.. http://dx.doi.org/10.1186/1752-153X-4-15.

Astudillo, P.D., Tiburcio, J., González, F.J., 2007. The role of acids and bases on the electrochemical oxidation of hydroquinone: hydrogen bonding interactions in acetonitrile. J. Electroanal. Chem. 604, 57–64.

Balzani, V., Credi, A., Venturi, M., 2009. Light powered molecular machines. Chem. Soc. Rev. 38, 1542–1550.

Brewster, T.P., Ding, W., Schley, N.D., Hazari, N., Batista, V.S., Crabtree, R.H., 2011. Thiocyanate linkage isomerism in a ruthenium polypyridyl complex. Inorg. Chem. 50, 11938–11946.

Brimblecombe, R., Koo, A., Dismukes, G.C., Swiegers, G.F., Spiccia, L., 2010. Solar driven water oxidation by a bioinspired manganese molecular catalyst. J. Am. Chem. Soc. 132, 2892–2894.

Campagna, S., Puntoriero, F., Nastasi, F., Bergamini, G., Balzani, V., 2007. Photochemistry and photophysics of coordination compounds: ruthenium. Top. Curr. Chem. 280, 117–214.

Castro, A.M., Delgado, J., Orellana, G., 2005. Hydrocarbon in water sensing with PTFE membranes doped with a luminescent Ru(II) poly(pyridyl) complex. J. Mater. Chem. 15, 2952–2958.

Chandrasekharam, M., Rajkumar, G., Rao, C.H.S., Suresh, T., Reddy, P.Y., Soujanya, Y., 2011. Ruthenium(II)- bipyridyl with extended π-system: improved thermo-stable sensitizer for efficient and long-term durable dye sensitized solar cells. J. Chem. Sci. 123, 555–565.

Chi, Y., Chou, P.T., 2010. Transition-metal phosphors with cyclometalating ligands: fundamentals and applications. Chem. Soc. Rev. 39, 638–655.

Chitra, S., Somasundaram, N., Easwaramoorthy, D., 2013. Ruthenium dyes with donor and acceptor moieties for TiO_2 solar cells. Arch. Appl. Sci. Res. 5, 112–119.

Cui, Y., Niu, Y.L., Cao, M.L., Wang, K., Mo, H.J., Zhong, Y.R., Ye, B.H., 2008. Ruthenium(II) 2,2′-bibenzimidazole complex as a second-sphere receptor for anions interaction and colorimeter. Inorg. Chem. 47, 5616–5624.

Dunn, B., Zink, J.I., 2007. Molecules in glass: probes, ordered assemblies and functional materials. Acc. Chem. Res. 40, 747–755.

Gianmaria, F.F., Ivana, A., Aniello, I., Armando, Z., Gabriele, P., Antonino, P., 2011. Plant polyphenols and their anti-cariogenic properties: a review. Molecules 16, 1486–1507.

Gill, M.R., Thomas, J.A., 2012. Ruthenium(II) polypyridyl complexes and DNA-from structural probes to cellular imaging and therapeutics. Chem. Soc. Rev. 41, 3179–3192.

Harris, C.S., Mo, F., Migahed, L., Chepelev, L., Haddad, P.S., Wright, J.S., Willmore, W.G., Arnason, J.T., Bennett, S.A.L., 2007. Plant phenolics regulate neoplastic cell growth and survival: a quantitative structure–activity and biochemical analysis. Can. J. Physiol. Pharmacol. 85, 1124–1138.

Holder, E., Langeveld, B.M.W., Schubert, U.S., 2005. New trends in the use of transition metal-ligand complexes for applications in electroluminescent devices. Adv. Mater. 17, 1109–1121.

Huili, W., Jingwen, M., Ailian, D., Baoguang, C., Wenwei, W., Meiping, M., Xuedong, W., 2012. Fuorescence quenching of 4-tert-octylphenol by room temperature ionic liquids and its application. J. Fluoresc., 10.1007/s10895-012-1150-1.

Kalyanasundaram, K., Graetzel, M., 2010. Artificial photosynthesis: biomimetic approaches to solar energy conversion and storage. Curr. Opin. Biotechnol. 21, 298–310.

Kavan, L., Exnar, I., Zakeeruddin, S.M., Grätzel, M., 2008. Molecular wiring of olivine $LiFePO_4$ by ruthenium(II)-bipyridine complexes and by their assemblies with single-walled carbon nanotube. J. Phys. Chem. C 112, 8708–8714.

Lakowicz, J.R., 2006. Principles of Fluorescence Spectroscopy, third ed. Springer Press, New York.

Lee, K.W., Slinker, J.D., Gorodetsky, A.A., Torres, S.F., Abruna, H.D., Houston, P.L., Malliaras, G.G., 2003. Photophysical properties of tris(bipyridyl)ruthenium(II) thin films and devices. Phys. Chem. Chem. Phys. 5, 2706–2709.

Li, M.J., Chen, Z., Yam, V.W., Zu, Y., 2008. Multifunctional ruthenium(II) polypyridine complex-based core-shell magnetic silica nanocomposites: magnetism, luminescence, and electrochemiluminescence. ACS Nano. 2, 905–912.

Li, L., Duan, L.L., Xu, Y.H., Gorlov, M., Hagfeldt, A., Sun, L.C., 2010. A photoelectrochemical device for visible light driven water splitting by a molecular ruthenium catalyst assembled on dye-sensitized nanostructured TiO_2. Chem. Commun. 46, 7307–7309.

Liao, G.L., Chen, X., Ji, L.N., Chao, H., 2012. Visual specific luminescent probing of hybrid G-quadruplex DNA by a ruthenium polypyridyl complex. Chem. Commun. 48, 10781–10783.

Lo, K.K., Lee, T.K., Lau, J.S., Poon, W.L., Cheng, S.H., 2008. Luminescent biological probes derived from ruthenium(II) estradiol polypyridine complexes. Inorg. Chem. 47, 200–208.

Matos, M.S., Holfkens, J., Gehlen, M.H., 2008. Static and dynamic biomolecular fluorescence quenching of porphyrin dendrimers in solution. J. Fluoresc. 18, 821–826.

Metera, K.L., Sleiman, H.A., 2007. Luminescent vesicles, tubules, bowls and star micelles from ruthenium bipyridine block copolymers. Macromolecules 40, 3733–3738.

Miedlar, K., Das, P.K., 1982. (Tris(2,2′-bipyridine)ruthenium(II)-sensitized photooxidation of phenols. environmental effects on electron transfer yields and kinetics. J. Am. Chem. Soc. 104, 7462–7469.

Mori, S.N., Kubo, W., Kanzaki, T., Masaki, N., Wada, Y., Yanagida, S., 2007. Investigation of the effect of alkyl chain length on charge transfer at TiO_2/dye/electrolyte interface. J. Phys. Chem. C 111, 3522–3527.

Rajendran, T., Rajagopal, S., Srinivasan, C., Ramamurthy, P., 1997. Micellar effect on the photoinduced electron-transfer reactions of ruthenium(II)-polypyridyl complexes with pnenolate ions. Effect of cetylammonium chloride. J. Chem. Soc. Faraday Trans. 93, 3155–3160.

Rajendran, T., Thanasekaran, P., Rajagopal, S., AllenGnanaraj, G., Srinivasan, C., Ramamurthy, P., Venkatachalapathy, B., Manimaran, B., Lu, L., 2001. Steric effects in the photoinduced electron transfer reactions of ruthenium(II)-polypyridine complexes with 2,6-disubstituted phenolate ions. Phys. Chem. Chem. Phys. 3, 2063–2069.

Ramamurthy, P., 1993. Build your data station for fast kinetic equipments. Chem. Educ. 9, 56–60.

Sannino, D., Vaiano, V., Ciambelli, P., Zama, I., Gorni, G., 2013. Evaluation of N719 amount in TiO_2 films for DSSC by thermogravimetric analysis. J. Therm. Anal. Calorim. 111, 453–458.

Schmittel, M., Lin, H., 2008. Electropolymerisable ruthenium(II) phenanthroline carrying azacrown ether receptors: metal ion recognition in thin film redox sensors. J. Mater. Chem. 18, 333–343.

Siebert, R., Winter, A., Schubert, U.S., Dietzek, B., Popp, J., 2011. Molecular mechanism of dual emission in terpyridine transition metal complexes – ultrafast investigations of photoinduced dynamics. Phys. Chem. Chem. Phys. 13, 1606–1617.

Sun, Y., Sibrina, N.C., Lauren, E.J., Turro, C., 2010. Unusual Photophysical properties of a ruthenium(II) complex related to $[Ru(bpy)2(dppz)]^{2+}$. Inorg. Chem. 49, 4257–4262.

Swarnalatha, K., Rajkumar, E., Rajagopal, S., Ramaraj, R., Lu, Y.L., Lu, K.L., Ramamurthy, P., 2005. Photoinduced electron transfer reactions of ruthenium(II) complexes containing 2,2′-bipyridine-4,4′-dicarboxylic acid with phenols Steric and charge effects. J. Photochem. Photobiol. A Chem. 171, 83–90.

Swarnalatha, K., Rajkumar, E., Rajagopal, S., Ramaraj, R., Banu, I.SP., Ramamurthy, P., 2011. Proton coupled electron transfer reaction of phenols with excited state ruthenium(II) – polypyridyl complexes. J. Phys. Org. Chem. 24, 14–21.

Tan, L.F., Liu, J., Shen, J.L., Liu, X.H., Zeng, L.L., Jin, L.H., 2012. First ruthenium(II)-polypyridyl complex as a true molecular "Light Switch" for triplex RNA structure: $[Ru(phen)(_2)(mdpz)]^{(2+)}$ enhances the stability of Poly(U)center dot Poly(A)(*)Poly(U). Inorg. Chem. 51, 4417–4419.

Tan, L.F., Xie, L.J., Sun, X.N., 2013. Binding properties of Ru(II) polypyridyl complexes with poly(U) poly(A)*poly(U) triplex: the ancillary ligand effect on third-strand stabilization. J. Biol. Inorg. Chem. 18, 71–80.

Thanasekaran, P., Rajagopal, S., Chockalingam, S., 1998. Photoredox reactions of tris(2,2′-bipyrazine)-, tris(2,2′-bipyrimidine)- and tris(2,3-bis[2-pyridyl] pyrazine)ruthenium(II) cations with phenolate ions in aqueous acetonitrile. J. Chem. Soc. Faraday Trans. 94, 3339–3344.

Trouillas, P., Marsal, P., Siri, D., Lazzaroni, R., Duroux, J.L., 2006. A DFT study of the reactivity of OH groups in quercetin and taxifolin antioxidants: The specificity of the 3-OH site. Food Chem. 97, 679–688.

Tuikka, M., Hirva, P., Rissanen, K., Tommola, J.K., Haukka, M., 2011. Halogen bonding – a key step in charge recombination of the dye-sensitized solar cell. Chem. Commun. 47, 4499–4501.

Verma, S., Tripathi, P.N., Rajesh, P.S., 2012. Marcus inverted region in the photoinduced electron transfer reactions of ruthenium(II)-polypyridine complexes with phenolate ions. Int. Multidiscip. Res. J. 2, 45–50.

White, T.A., Knoll, J.D., Arachchige, S.M., Brewer, K.J., 2012. A series of supramolecular complexes for solar energy conversion via water reduction to produce hydrogen: an excited state kinetic analysis of Ru(II), Rh(III), Ru(II) photoinitiated electron collectors. Materials 5, 27–46.

Xu, J., Wu, H., Jia, X., Zou, D., 2012. A dendron modified ruthenium complex: enhanced open circuit voltage in dye-sensitized solar cells. Chem. Commun. 48, 7793–7795.

Young, K.J., Martini, L.A., Milot, R.L., Snoeberger, R.C., Batista, V.S., Schmuttenmaer, C.A., Crabtree, R.H., Brudvig, G.W., 2012. Light-driven water oxidation for solar fuels. Coord. Chem. Rev. 256, 2503–2520.

Zhu, K., Jang, S.R., Arthur, J., 2012. Frank effects of water intrusion on the charge-carrier dynamics, performance, and stability of dye-sensitized solar cells. Energy Environ. Sci. 5, 9492–9495.